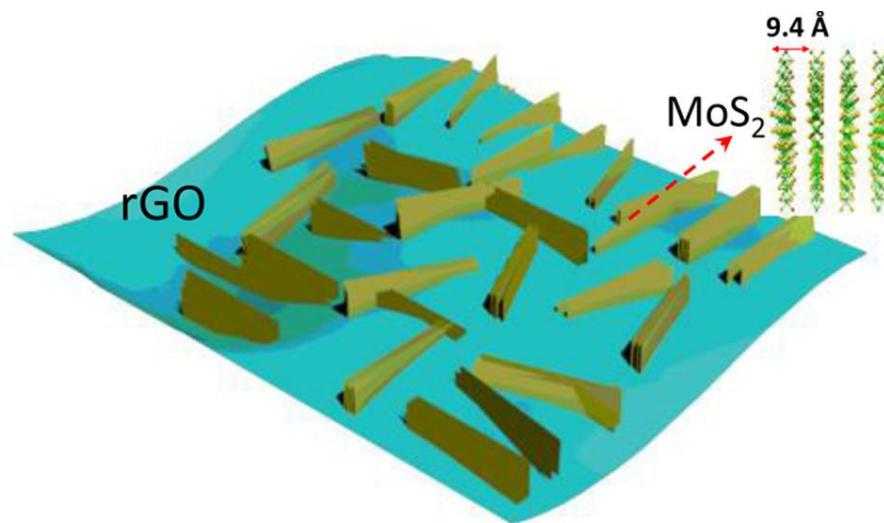


## Enabling Colloidal Synthesis of Edge-Oriented MoS<sub>2</sub> with Expanded Interlayer Spacing for Enhanced HER Catalysis

Yugang Sun,<sup>\*,†</sup> Farbod Alimohammadi,<sup>†</sup> Dongtang Zhang,<sup>†,‡</sup> and Guangsheng Guo<sup>‡</sup>

<sup>†</sup>Department of Chemistry, Temple University, 1901 North 13th Street, Philadelphia, Pennsylvania 19122, United States

<sup>‡</sup>Beijing Key Laboratory for Green Catalysis and Separation, Department of Chemistry and Chemical Engineering, Beijing University of Technology, Beijing, 100124, People's Republic of China



# Introduction :

- ❖ Increasing catalytic activity of non-Pt nanomaterials (e.g., oxides, chalcogenides, organic–inorganic complex, and so forth.) toward electrochemical hydrogen evolution reaction (HER) represents a challenging but promising research direction because of the importance of hydrogen production in clean energy applications.
- ❖ In this direction, nanostructured MoS<sub>2</sub> has been actively explored as an inexpensive catalyst to promote HER in recent years.
- ❖ Previous work has highlighted the importance of the intrinsic structural parameters including crystalline phase, edge site density/orientation and interlayer spacing on determining HER catalytic activity of MoS<sub>2</sub> nanostructures.  

For example, highly conducting 1T-phase MoS<sub>2</sub> sheets (metallic octahedral structure) exhibit improved HER catalytic activity compared to the semiconducting 2H-phase MoS<sub>2</sub> sheets (semiconducting trigonal prismatic structure) because both edges and basal surfaces in 1T MoS<sub>2</sub> are catalytically active whereas only the edges of 2H MoS<sub>2</sub> are active.
- ❖ However, the significant instability of the 1T MoS<sub>2</sub> prevents its wide use in HER applications. As for the structurally stable 2H MoS<sub>2</sub>, HER activity can be enhanced by either exposing high density of active MoS<sub>2</sub> edges or expanding the interlayer spacing of MoS<sub>2</sub> nanostructures.

- ❖ It is even more promising to fabricate nanostructured MoS<sub>2</sub> that can simultaneously exhibit both high-density edges and expanded interlayer spacing, which can synergistically improve HER activity of the MoS<sub>2</sub>.

## **Previous reports :**

- ❖ Wang et al. reported an approach relying on rapid sulfurization of thin ALD Mo films with hot S vapor, which produces MoS<sub>2</sub> nanostructures with well-aligned edge-oriented (EO) geometry, which is favorable for pulling electrons from underneath support electrode (due to the high inlayer conductivity) to the active edge sites to promote HER.
- ❖ In addition, intercalation of lithium in the EO MoS<sub>2</sub> can expand the van der Waals gaps to further increase its HER performance in terms of enhanced current density and reduced Tafel slope.
- ❖ Only a few successful examples have been reported for the synthesis of EO & IE MoS<sub>2</sub> with normal interlayer spacing (i.e.,  $\sim 6.2 \text{ \AA}$ ) through gas-phase sulfurization of thin Mo and Mo oxide films. The solid-vapor phase synthesis is costly, difficult to scale up.

## **In this Paper :**

Selectively promoted heterogeneous nucleation/growth of MoS<sub>2</sub> on graphene monolayer sheets. The MoS<sub>2</sub> nanosheets were edge oriented (EO) with expanded interlayer spacing ( $\sim 9.4$  Å) supported on reduced graphene oxide (rGO) sheets and successfully synthesized through colloidal chemistry, showing the promise in low-cost and large-scale production.

## **Synthesis of EO & IE MoS<sub>2</sub> :**

3 mg of GO nanosheets was dispersed in 6 mL of DMF with assistance of ultrasonication for 0.5 h.

To this dispersion was added 10 mg of (NH<sub>4</sub>)<sub>2</sub>MoS<sub>4</sub>, which was dissolved with assistance of magnetic stirring for 20 min under ambient condition.

The DMF dispersion containing both GO and (NH<sub>4</sub>)<sub>2</sub>MoS<sub>4</sub> was transferred to a 10 mL reaction vessel that was sealed and placed in a microwave reactor . The dispersion was then quickly heated to an appropriate temperature (e.g., 200, 220, 240, and 260 °C) in a period of  $\sim 10$  s and the temperature was maintained for 2 h to complete the reaction.

The products were then collected via centrifugation followed by washing with DI water and ethanol and then dried in an oven.

# Results and discussions :

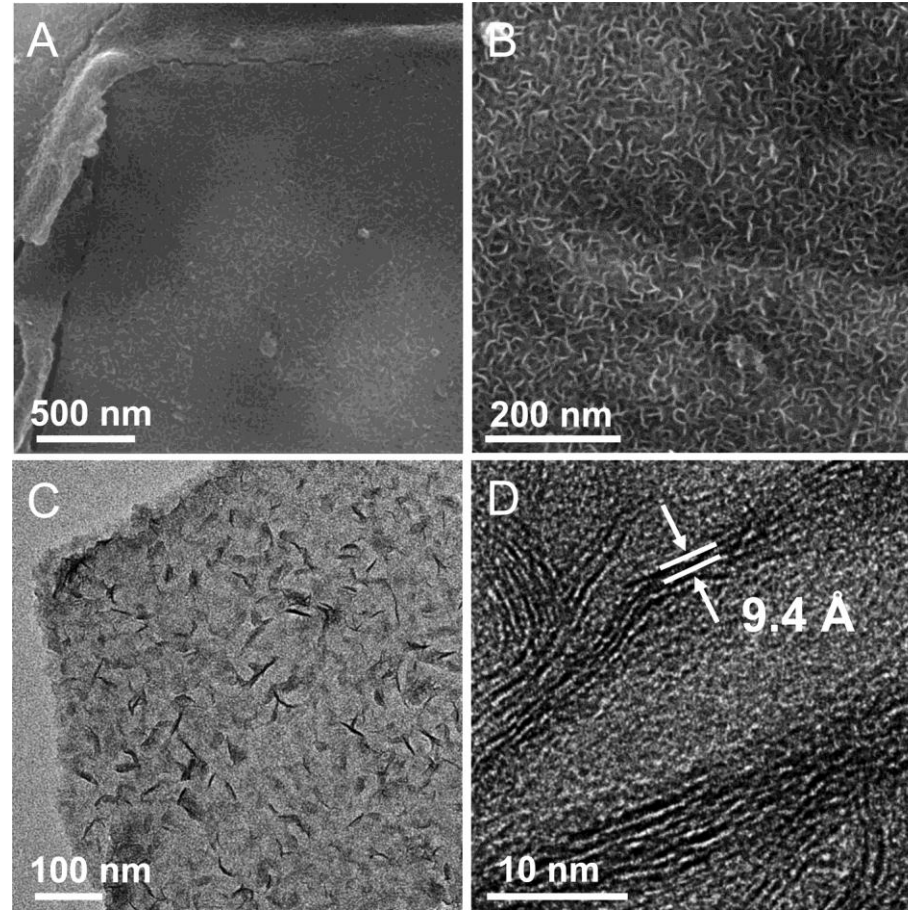


**Figure 1.** (A,B) SEM and (C) TEM images of EO&IE MoS<sub>2</sub>/rGO sample synthesized from a reaction at 260 °C for 2 h. (D) HRTEM image of several EO&IE MoS<sub>2</sub> nanosheets on a rGO nanosheet, highlighting the layered structure and exposed edges in the MoS<sub>2</sub> nanosheets.

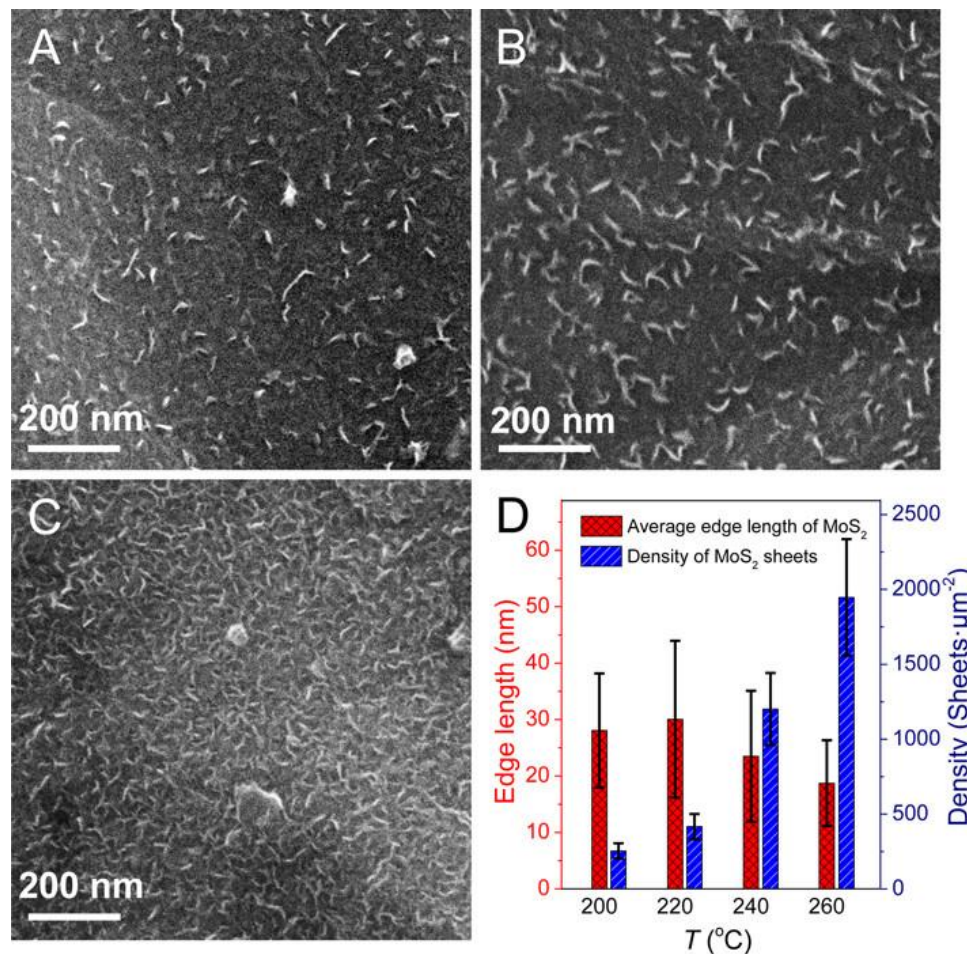


**Figure 2.** SEM images of EO&IE MoS<sub>2</sub>/rGO synthesized from reactions at different temperatures: (A) 200 °C, (B) 220 °C, and (C) 240 °C. The reaction time was 2 h. (D) Statistic analysis of the number of MoS<sub>2</sub> nanosheets on 1  $\mu\text{m}^2$  rGO surface (blue columns) and the average edge length of one MoS<sub>2</sub> nanosheet (red columns).

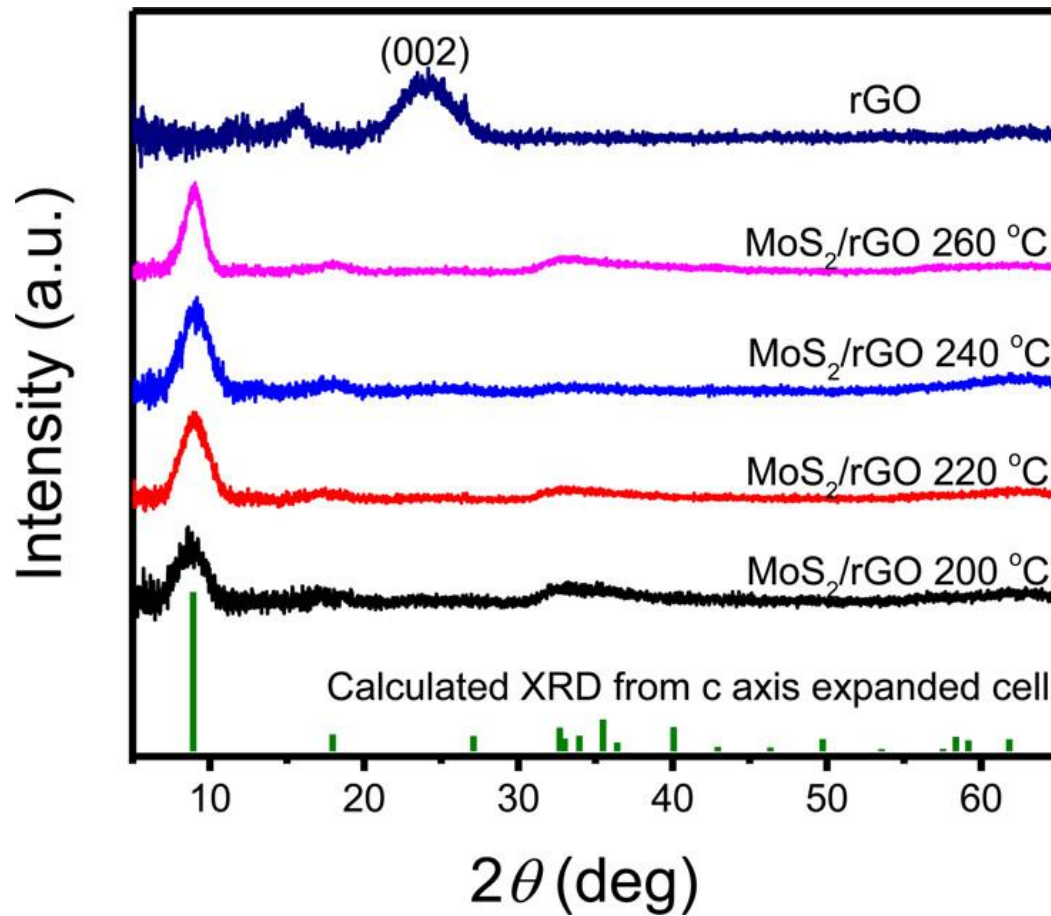


**Figure 3.** X-ray diffraction patterns of EO&IE MoS<sub>2</sub>/rGO synthesized from reactions at different temperatures. The calculated pattern a MoS<sub>2</sub> lattice with expansion along the c-axis is plotted for reference (green curve).

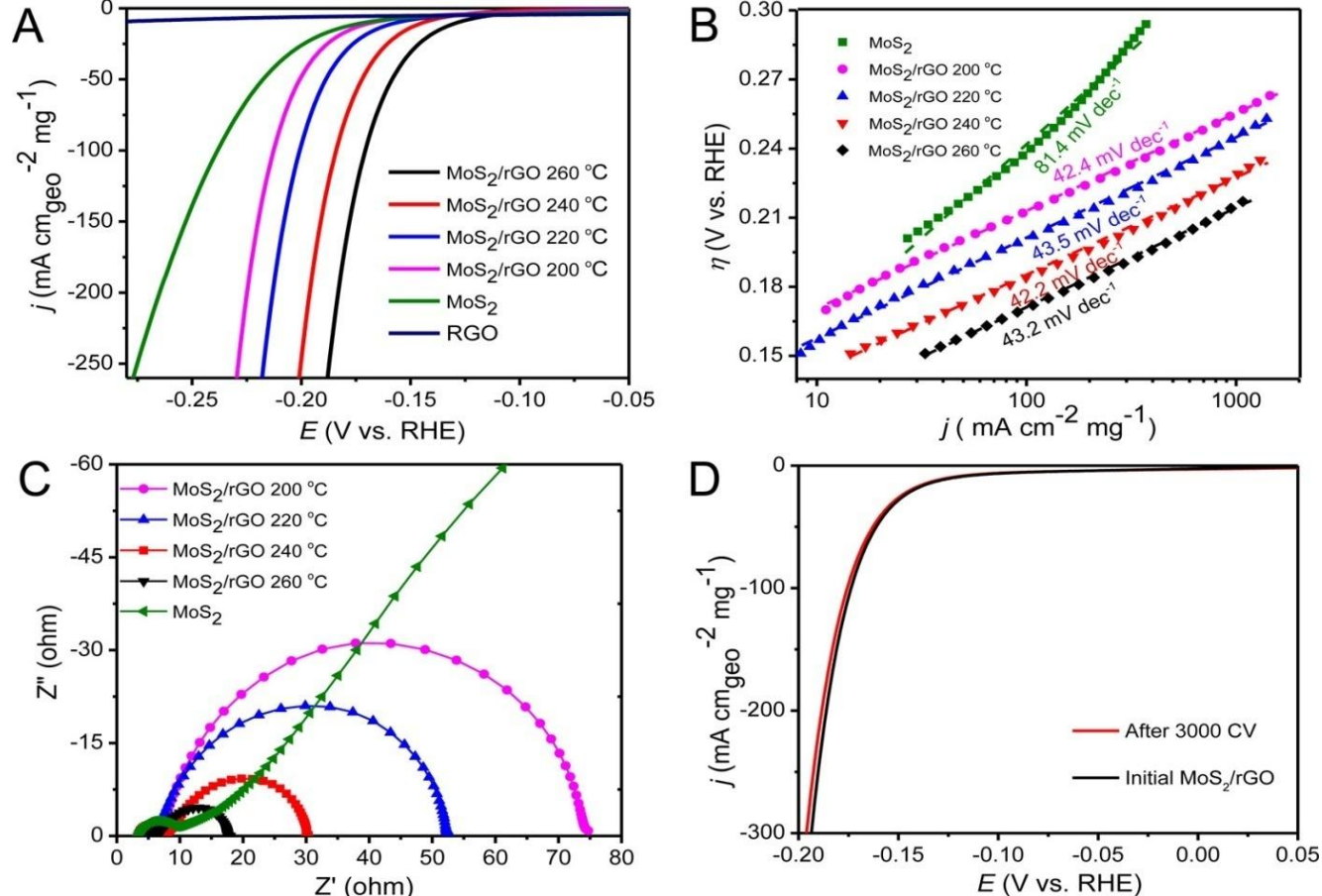


**Figure 4.** (A) Normalized polarization curves for HER on modified glassy carbon electrodes comprising EO&IE MoS<sub>2</sub>/rGO catalysts synthesized at different temperatures, IE MoS<sub>2</sub> microflowers and rGO sheets synthesized at 220 °C. The potential sweep rate was 5 mV s<sup>-1</sup>. (B) Tafel plots and (C) Nyquist plots of the corresponding catalysts of (A). (D) Comparison of polarization curves of the EO&IE MoS<sub>2</sub>/rGO sample synthesized at 260 °C before (black) and after (red curve) 3000 potential cycles between -0.3 and 0.3 V versus RHE at a sweep rate of 200 mV s<sup>-1</sup>.



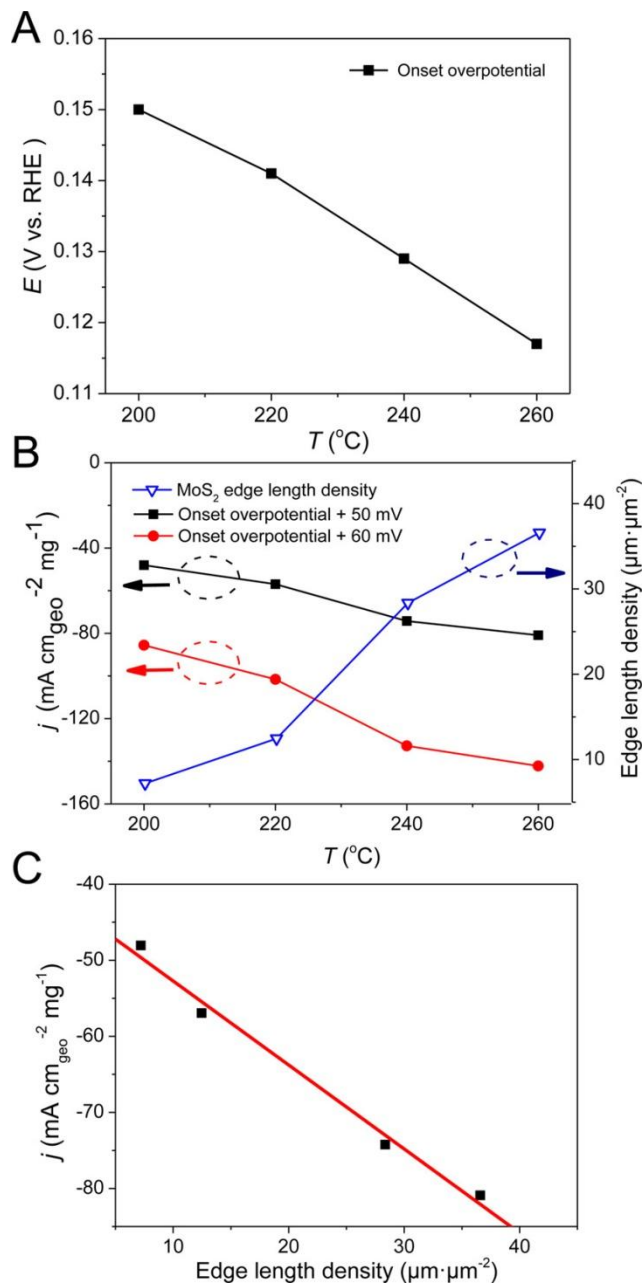


**Figure 5.** (A) Onset overpotentials required to initiate HER for EO&IE MoS<sub>2</sub>/rGO synthesized at different temperatures. (B) Current density at the same offset overpotential for different EO&IE MoS<sub>2</sub>/rGO catalysts. The MoS<sub>2</sub> edge length density (i.e., total MoS<sub>2</sub> edge length with unit of  $\mu\text{m}$  on  $1 \mu\text{m}^2$  rGO surface) of different catalysts are also plotted for comparison. (C) The linear relationship between current density and the MoS<sub>2</sub> edge length density for the EO&IE MoS<sub>2</sub>/rGO catalysts.

## Summary :

- ❖ By taking advantage of unique heterogeneous nucleation and growth processes of MoS<sub>2</sub> on GO sheets and the unique reaction kinetics in the microwave solvothermal reaction, MoS<sub>2</sub> nanosheets with expanded interlayer spacing of 9.4 Å have been successfully grown on rGO sheets to show EO geometry that effectively exposes catalytically active MoS<sub>2</sub> edges toward electrolyte.
- ❖ The edge-oriented and interlayer-expanded (EO&IE) MoS<sub>2</sub>/rGO exhibited significantly improved catalytic activity toward hydrogen evolution reaction (HER) in terms of larger current density, lower Tafel slope, and lower charge transfer resistance compared to the corresponding interlayer-expanded MoS<sub>2</sub> sheets without edge-oriented geometry.
- ❖ These understandings shed light on rational design of high-performance HER catalysts that can be achieved by controlling nucleation and growth kinetics of colloidal chemistry.